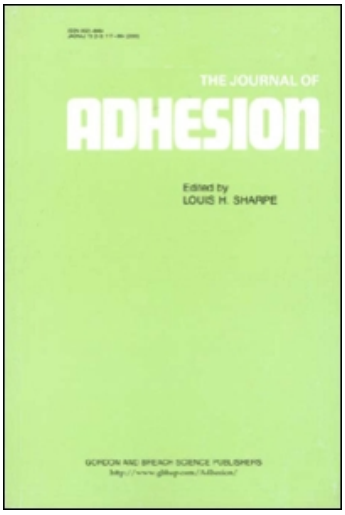

The Journal of Adhesion
Publication details, including instructions for authors and subscription information:
http://www.informaworld.com/smpp/title~content=t713453635

Residual Stress Development in Adhesive Joints Subjected to Thermal Cycling

G. Robert Humfeld Jr.[a]; David A. Dillard[a]
[a] Department of Engineering Science and Mechanics, Virginia Polytechnic Institute and State University, Blacksburg, Virginia, USA

To cite this Article Humfeld Jr., G. Robert and Dillard, David A.(1998) 'Residual Stress Development in Adhesive Joints Subjected to Thermal Cycling', The Journal of Adhesion, 65: 1, 277 — 306
To link to this Article: DOI: 10.1080/00218469808012250
URL: http://dx.doi.org/10.1080/00218469808012250

J. Adhesion, 1998, Vol. 65, pp. 277–306
Reprints available directly from the publisher
Photocopying permitted by license only

Residual Stress Development in Adhesive Joints Subjected to Thermal Cycling

G. ROBERT HUMFELD JR. and DAVID A. DILLARD*

Department of Engineering Science and Mechanics, Virginia Polytechnic Institute and State University, Blacksburg, Virginia 24061-0219, USA

(Received 30 October 1996; In final form 11 August 1997)

The effect of thermal cycling on the state of residual stress in thermoviscoelastic polymeric materials bonded to stiff elastic substrates was investigated using numerical techniques, including finite element methods. The work explored the relationship between a cyclic temperature environment, temperature-dependent viscoelastic behavior of polymers, and thermal stresses induced in a bimaterial system. Due to the complexity of developing a closed-form solution for a system with time- and temperature-dependent material properties, and time-varying temperature and coupled boundary conditions, numerical techniques were used to acquire approximate solutions.

The results indicate that residual stresses in an elastic-viscoelastic bimaterial system incrementally shift over time when subjected to thermal cycling. Potentially damaging tensile axial and peel stresses develop over time as a result of viscoelastic response to thermal stresses induced in the polymeric layer. The applied strain energy release rate at the ends of layered or sandwich specimens is shown to increase as axial stress develops. The rate of these changes is dependent upon the thermal cycling profile and the adhesive's thermo-mechancial response. Discussion of the results focuses on the possiblility that the increasing tensile residual stresses induced in an adhesive bond subjected by thermal cycling may lead to damage and debonding, thus reducing bond durability.

Keywords: Thermal cycling; adhesive bond; coatings; polymer; time/temperature superposition; stress relaxation; residual stress; thermal stress; viscoelasticity; thermo-viscoelasticity; thermal ratchetting

*Corresponding author.

INTRODUCTION

Changes in temperature affect adhesive bonds by inducing thermal stresses in the system and by changing the mechanical properties of the viscoelastic adhesive. This paper investigates the interaction between these effects and identifies an evolution of residual stresses toward a more tensile stress state as a result of cyclic thermal exposure. Such changes in the residual stress state could potentially reduce the useful life of adhesive bonds and polymeric materials in a variety of applications.

The study was prompted by reports from industry contacts that cyclic thermal testing was leading to spontaneous failure of adhesive sandwich specimens. The specimens were observed to remain sound for an initial period of thermal cycling, until cracks developed along each interface at the free edges. The length of the debonds steadily grew as thermal cycling continued. Furthermore, the debonded portions of the adhesive layer were noticeably shorter than the original bond. Once completely debonded and separated from the substrates, the adhesive layer was observed to be significantly shorter (Fig. 1). Neat polymer specimens subjected to identical thermal loading were reported to have undergone no similar dimensional changes, suggesting that the polymer shrinkage was related to the bimaterial system.

The authors hypothesize that the observed behavior in the bonded system is due to the fluctuating mechanical behavior of the polymer during thermal cycling. Debonding is believed to be caused by thermal stresses resulting from a mismatch of the coefficients of thermal expansion (CTE) of the adhesive and substrate(s). In some material systems, these stresses will be shown to increase in severity as a result of thermal cycling exposure. Contraction of the adhesive layer after or during debonding is believed to be evidence of viscoelastic flow

FIGURE 1 Contraction of the adhesive layer after debonding due to thermal cycling.

occurring in the adhesive during thermal exposure. Were other changes in the adhesive (*i.e.* volume loss, aging, decomposition, etc.) responsible, contraction should also have been evident in the neat specimen. (Frictional effects are also believed to play a role in the large amounts of shrinkage observed, but will be the topic of a future paper.)

Background

Thermal and residual stresses have been the subject of much study in the last 70 years. Thermal stresses in bimetal systems have been widely examined, first by Timoshenko [1] in 1925. Analyses of increasing complexity followed, considering systems with interfacial cracking [2], more complicated geometries [3], and transverse stress considerations [4, 5]. These works all report that altering the temperature of a bimetal strip induces axial stresses in the system components – tensile in one and compressive in the other. These stresses run parallel to the interface with nearly constant magnitudes along most of the center region and a drop off to zero near the edges. Shear stresses were found to be zero along the interface except near the edges, where they reach a maximum. Analysis of transverse stresses by Suhir [4, 5] predicted high tensile peel stresses at the free edges, with small compressive regions between the ends and a large region in the middle of the bond with no significant peel stresses, closely resembling classical beam-on-elastic-foundation solutions. All of these analyses applied to systems containing no components with time- or temperature-dependent material properties.

Investigation of temperature- and time-dependent behavior of polymeric material systems subjected to thermal changes is widely available. A good analytical overview can be found in a paper by Losi and Knauss [6]. Struik's experimental study of "frozen-in" deformations in polymers [7] is directly relevant to this study. He applied a constant creep stress to polymer specimens while subjecting them to changing temperature. Creep compliance and recovery predictions by analysis similar to that used in this paper were found to match experimental results reasonably well. The reader may also be interested in works relating to cooling and curing stresses [8, 9, 10], some of which include consideration of thermal conduction, a factor neglected in this paper for simplicity.

Thermal cycling as a source of damage in material systems has been reported for a wide variety of situations. Failure in plastic packaging [11], solder joints [12], and thermal barrier films [13] has been attributed to thermal cycling, but without specific mechanisms of failure being identified. Thermal fatigue [14] and thermal ratchetting [15] are two failure mechanisms that have been identified in materials subjected to thermal cycling – the former describing incremental crack growth in constrained materials and the latter defining plastic strain accumulation in metals cycled at very high temperatures. An analytical study of the effect of thermal cycling on elastic bimaterial systems has been presented by Ryan and Mall [16].

Thermal cycling effects and non-linear material response are considered together in some works. A paper by Suresh [17] contains closed-form and finite element elasto-plastic analyses of layered materials subjected to thermal cycling. Inelastic strain accumulation in short fiber metal matrix composites during thermal cycling has been considered by Dunn and Taya [18]. A study of the thermoviscoelastic response of graphite/epoxy composites during thermal cycling has been authored by Lin and Huang [19]. However, a definitive treatment of the problem of a viscoelastic-elastic bimaterial system subjected to thermal cycling does not appear to exist in the current body of literature.

This work is an attempt to add to the current understanding of thermal and residual stress development in polymeric coatings and adhesive bonds by considering the effects of temperature-dependence and viscoelastic flow during thermal cycling of a bimaterial system. An understanding of the development of stress over time at an elastic-viscoelastic bimaterial interface subjected to a cyclic thermal profile could contribute to more effective design and failure analysis for a wide variety of applications and is, therefore, of compelling interest and importance for the adhesives and coatings industries, as well as other areas in which polymers are attached to other materials.

PROBLEM DEFINITION

The problem considered is that of a polymeric layer bonded to one substrate as a coating or between two substrates as an adhesive. The

substrate material is assumed to be elastic and relatively stiff (*e.g.* a metal). The polymeric adhesive or coating is assumed to be a thermorheologically simple, linear viscoelastic, non-aging, isotropic material. The entire system is subjected to a cyclic temperature profile (*e.g.* square-wave, sine-wave) and expands and contracts with the changes in temperature. The CTE mismatch induces in-plane strains and stresses throughout the layers; these stresses in turn result in concentrations of shear and peel stresses near the interface edges. Because of the complexities involved, numerical solutions are obtained.

For the solutions presented, thermal conduction was assumed to be an instantaneous process, resulting in spatially-uniform temperatures (and therefore thermal strains) throughout. The coefficient of thermal expansion was assumed to be temperature dependent, but independent of time. Because the material system of interest involved a room temperature cure adhesive, the bond was assumed to be stress-free (at room temperature) before any thermal cycling was applied. (Although this stress-free assumption affects the starting point for the stress evolution, it does not affect the final stress state which develops for a given system.) Other assumptions were made in each of the solution approaches and are explained in the appropriate sections. We now present the analysis of two geometries, the first a 1-D bar model developed to study the in-plane stress evolution, and the second, a 2-D finite element representation of the geometry.

THERMOVISCOELASTIC ANALYSIS OF A 1-D BAR

Geometry

As noted in a previous section, the normal stress parallel to the bond plane is relatively uniform away from the ends of bimaterial bonds. In an effort to simplify the geometry to focus on the time-dependent evolution of these stresses, we model the polymeric layer in a narrow adhesive bond as a viscoelastic bar with constraints preventing any thermal expansion or contraction in the axial direction (Fig. 2). The effective coefficient of thermal expansion is taken as the difference in thermal expansions of the polymer layer and the relatively stiff

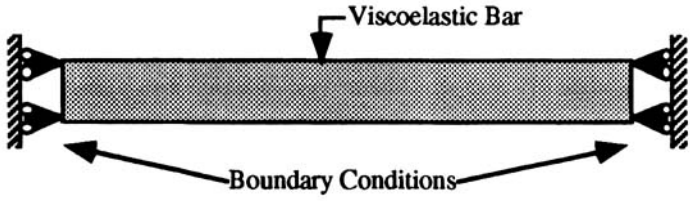

FIGURE 2 Axially-constrained viscoelastic bar.

substrate(s). This simplification has constraints similar to those in the center of a typical sandwich bond geometry and is useful because it focuses on the influence of viscoelastic relaxation on the stresses induced by thermal cycling independent of geometry dependencies. Analysis is simpler because stress is one-dimensional, uniform along the length of the bar, and induced by constraints acting independent of time and temperature. The results will give important insights into problems with more complicated boundary conditions such as the bimaterial system.

Derivation of the Recursive Equation

The Maxwell element (Fig. 3) was selected as the mechanical model for this material because the problem most nearly resembles a stress relaxation problem. The derivation that follows builds on the work of Zienkiewicz *et al.* for a Kelvin element [20]. Using standard notation, the governing differential equation for a Maxwell element may be written as:

$$\dot{\sigma} + \frac{E}{\eta}\sigma = E\dot{\varepsilon} \tag{1}$$

where $\dot{\varepsilon}$ is defined as the time-derivative of the mechanical strain.

Total strain in this system is the sum of two components: mechanical strain (ε_M) and thermal strain (ε_T). Given that the

FIGURE 3 Single Maxwell element representation.

constrained bar has fixed ends, the sum must always be zero; mechanical strain is equal and opposite to the thermal strain. $\dot{\varepsilon}$ is therefore:

$$\dot{\varepsilon} = \frac{\partial \varepsilon_M}{\partial t} = -\frac{\partial \varepsilon_T}{\partial t} = -\alpha(T(t))\frac{dT(t)}{dt} \tag{2}$$

Let σ_i be the stress at any time $t = t_i$; we can determine the stress σ_{i+1} at $t = t_i + \Delta t$ by integrating the governing differential Eq. (1)

$$\int_{\sigma_i}^{\sigma_{i+1}} d\sigma = \int_{t_i}^{t_i+\Delta t} \left[E\dot{\varepsilon} - \frac{E}{\eta}\sigma(t)\right] dt \tag{3}$$

If we assume that $\dot{\varepsilon}$ is constant over a small time step Δt, integration yields the equation

$$\sigma_{i+1} - \sigma_i = E\dot{\varepsilon}\Delta t - \frac{E}{\eta}\int_{t_i}^{t_{i+\Delta t}} \sigma(t)dt. \tag{4}$$

The assumption that $\dot{\varepsilon}$ is constant over Δt will control how small Δt must be for a given temperature profile to obtain a reasonably accurate solution.

Stress as a function of time can be determined from the governing differential equation (again assuming that $\dot{\varepsilon}$ is constant):

$$\sigma(t) = Ae^{\frac{-t}{\tau}} + \eta\dot{\varepsilon} \tag{5}$$

Where $\tau = \frac{\eta}{E}$ is the characteristic relaxation time of the Maxwell element and A is a constant determined by the initial condition $\sigma(t_i) = \sigma_i$:

$$A = \frac{\sigma_i - \eta\dot{\varepsilon}}{e^{\frac{-t_i}{\tau}}} \tag{6}$$

Completing the integration of $\sigma(t)$ and rearranging the resulting equation yields the recursive relation:

$$\sigma_{i+1} = \sigma_i e^{\frac{-\Delta t}{\tau}} + \eta\dot{\varepsilon}_i(1 - e^{\frac{-\Delta t}{\tau}}) \tag{7}$$

In order to account for viscoelastic temperature-dependence, the time variables are scaled by the temperature shift factor a_T, giving the

final form of the equation:

$$\sigma_{i+1} = \sigma_i e^{\frac{-\Delta t}{a_T \tau}} + a_T \eta \dot{\varepsilon}_i \left(1 - i e^{\frac{-\Delta t}{a_T \tau}}\right) \tag{8}$$

The shift factor a_T is the ratio of "reduced time" to real time for a material as a function of temperature. It can be taken directly from experimental data or modeled using any one of several available methods.

Equation (8) is a recursive relationship which can be used to track the development of stress over time by using a time-stepping process. It can be used with any temperature profile, but is only valid for the completely-constrained geometry. The stability and accuracy of the solution are determined by the size of the time step. If the time step is selected to be small enough to insure that $\dot{\varepsilon}$ is nearly constant for every increment Δt, then stable and reasonably accurate solutions are obtained.

This derivation can easily be extended to a generalized Maxwell element. Total stress in a generalized Maxwell element is the sum of the stresses in all components. Each component is subjected to the same strain profile, so each is independently governed by the recursive equation derived above. The equation for a generalized Maxwell element is, therefore, a summation of recursive equations of all of its elements:

$$\sigma_{i+1} = \sum_{j=1}^{n} \sigma_{i+1}^{(j)} = \sum_{j=1}^{n} \left[\sigma_i^{(j)} e^{\frac{-\Delta t}{a_T \tau^{(j)}}} + a_T \eta^{(j)} \dot{\varepsilon}_i \left(1 - e^{\frac{-\Delta t}{a_T \tau^{(j)}}}\right) \right] \tag{9}$$

where j represents the element number, n is the total number of elements, and $\dot{\varepsilon}_i$ is defined by evaluating Equation (2) at $t = t_i$. For the purposes of this paper, only a single Maxwell element will be needed to illustrate the thermal rachetting behavior which results.

Example Results

The recursive equation (Eq. (8)) was used to predict stress development in a constrained viscoelastic bar with the following material properties:

$E = 1\text{GPa}$
$\eta = 1$ GPa sec at T_g
$T_g = 87°\text{C}$

The CTE was assumed to be 100×10^{-6} °C^{-1} in the glassy region and 200×10^{-6} °C^{-1} in the rubbery region, with the actual dependence defined by the equation:

$$\alpha(T) = 50 \times 10^6 \left(3 + \text{Tanh}\left[\frac{3}{5}(T - T_g)\right]\right) \tag{10}$$

The Williams-Landel-Ferry (WLF) [21] equation was used to model the temperature shift factor:

$$\text{Log}\, a_T = \frac{C_1(T - T_g)}{C_2 + T - T_g} \tag{11}$$

and the constants $C_1 = 20$ and $C_2 = 100$°C were assumed in the analysis. The WLF equation is not strictly appropriate for temperatures below the glass transition temperature, but it was used because it is convenient for illustration purposes. More accurate representations of the temperature dependence would alter the stress evolution somewhat, but are not expected to change the trends and observations significantly.

The temperature profile applied was that of a symmetric, near-square wave cycling between $T_0 = 27$°C and $T_1 = 70$°C with a period of one hour, each cycle defined by the equation:

$$T(t) = 27 + 21.5\left[\text{Tanh}\left[\frac{t - 900}{120}\right] - \text{Tanh}\left[\frac{t - 2700}{120}\right]\right] \tag{12}$$

It will be noticed that Equation (12) is not a cyclic function; each cycle of the function was defined so that for any integer n,

$$T(n3600 \leq t \leq (n+1)3600) = T(0 \leq t \leq 3600)$$

(This smoothed square wave was used to avoid the anomalous spikes which result from the unit step functions involved in a true square wave. Due to the time required for thermal conduction, bonds would not typically experience a perfect square wave temperature profile.)

A Mathematica[1] program was developed to evaluate the solution using a time step (Δt in Eq. (8)) of 20 seconds. Convergence was confirmed by comparing with solutions using a time step of 1 second; over the course of 108,000 seconds, there was less than one percent difference between the solutions.

The results of the recursive solution method are presented below; stress in the axially-constrained polymer is plotted against time for three thermal cycles (Fig. 4) and 50 thermal cycles (Fig. 5). Stress is shown to increase incrementally in the axially-constrained bar over a number of cycles. In each cycle, increasing the temperature induces a compressive axial stress in the bar because thermal expansion is prevented by the end constraints. These compressive stresses relax at an accelerated rate due to the increased temperature. When the material is cooled, stress relaxation at the hot temperature is reflected in increased residual tensile stresses at the cold temperature. These stresses cannot be fully relieved before the next cycle begins because of the slow rate of relaxation at colder temperatures. Each full temperature cycle, therefore, results in an increased tensile residual stresses at the low temperature, a situation which may eventually cause or contribute to bond failure.

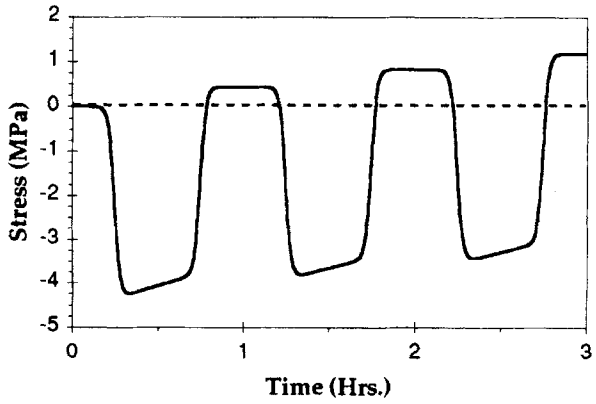

FIGURE 4 Stress development over 3 thermal cycles.

[1]Mathematica is a mathematics software tool developed by Wolfram Research Inc.

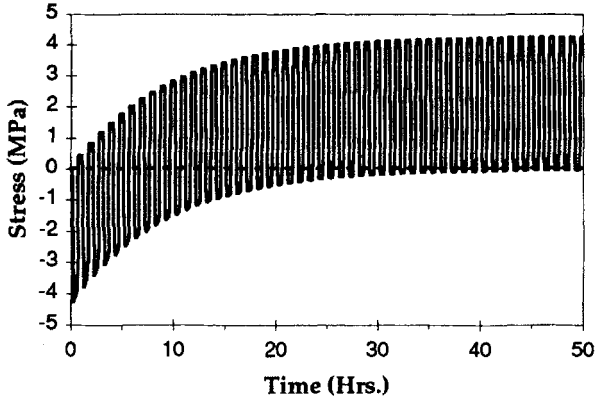

FIGURE 5 Stress development over 50 thermal cycles.

The reader is reminded that the trends here are more important than the exact magnitudes of stress in this example. Different systems would have different material properties, resulting in different stress levels. However, the trend of tensile stress development in viscoelastic adhesives during thermal loading is one that should be universal because it is a consequence of the fundamental mechanics of viscoelastic materials. It is also important to note that it is the time at elevated temperature which causes the shift in stresses, not the thermal cycling *per se*. The importance of the thermal cycling is simply that rather than obtaining reduced stresses due to stress relaxation, the temperature change can result in sign reversals of the stress. Thus, a relaxation of compressive stresses at elevated temperature leads to more severe tensile stresses at the lower service temperature.

Steady-State Analysis

Note in Figure 5 that tensile residual stress in the adhesive layer at the cold temperature asymptotically levels off over time. The value of the asymptote represents the maximum stress level that could develop in the specimen due to the given thermal profile; it occurs if the material reaches steady-state thermoviscoelastic oscillation. Whether stress ever reaches the steady-state asymptote value depends upon the properties of the polymer, the thermal history, and the time in the cycling environment. Although it may never be truly realized, the steady-state

cycle is useful to consider because it corresponds to the worst-case scenario for tensile stress development for a given problem.

For a material system at steady-state, the cumulative change in stress over a complete thermal cycle (of period P) is zero:

$$\int_t^{t+P} E(\xi - \xi')\alpha(T(\tau))\frac{\partial T(\tau)}{\partial \tau}d\tau = 0 \tag{13}$$

where $\xi(x,t) = \int_{(-\infty)}^{t} a_T(T(x,\zeta)\,d\zeta$ and $\xi' x,\tau = \int_{(-\infty)}^{\tau} a_T(T(x,\zeta))d\zeta$ are the reduced times. Determining the stress magnitudes using this relationship for arbitrary materials and thermal profiles is not straightforward. The case of a single Maxwell element subjected to a square-wave thermal profile is easily solved, however, and is presented below.

For a square wave thermal profile, there are instantaneous jumps in strain (since the CTE is not time-dependent) and shift factor, thus simplifying the hereditary integral:

$$\sigma_{h_0}(1 - e^{\frac{-P}{(2a_{T_h}\tau)}}) + \sigma_{c_0}(1 - e^{\frac{-P}{(2a_{T_c}\tau)}}) = 0 \tag{14}$$

where the new variables are defined:

σ_{h_0} instantaneous initial value of stress at the hot temperature
σ_{c_0} instantaneous initial value of stress at the cold temperature
a_{T_h} shift factor at the hot temperature
a_{T_c} shift factor at the cold temperature

The difference in the initial stress magnitudes (see Fig. 6) is

$$\sigma_{c_0} - \sigma_{h_0} = \delta\sigma_T + \delta\sigma_h \tag{15}$$

where the new variables are defined:

$\delta\sigma_T$ change in thermal stress for one jump
$\delta\sigma_h$ change in stress at hot temperature due to relaxation

The total change in stress magnitude for one stress ramp will depend upon the thermal profile. $\Delta\sigma_T$ is normally time-dependent and evaluated using Equation (3) over one thermal ramp. For a square-wave thermal profile in which temperature rises nearly instanta-

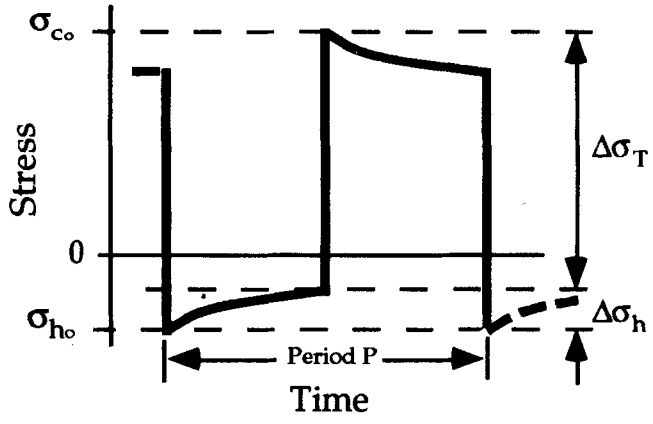

FIGURE 6 Closed stress *vs.* time loop achieved during steady state cycling.

neously, thermal stress can be expressed merely as a function of temperature. If thermal loading is truly instantaneous, no relaxation can occur during ramping; thermal stress would be a product of thermal strain and the glassy modulus. In order to take a temperature-dependent modulus into account, the one-second modulus was used in the integral to determine change in thermal stress during one temperature ramp. Solving Equation (15) for the cold-temperature stress yields:

$$\sigma_{c_0} = \frac{\int_{T_c}^{T_h} E_{1\text{sec}}(T)\,\alpha(T)\,dT}{\left[2 - e^{\frac{-P}{2a_{T_c}\tau}} - \left(\frac{1-e^{\frac{-P}{2a_{T_c}\tau}}}{1-e^{\frac{-P}{2a_{T_h}\tau}}}\right)\right]} \tag{16}$$

Equation (16) predicts a stress of 4.30 Mpa for the example material. This is very close to the maximum value of 4.27 MPa returned by the recursive equation (predicted by evaluating until very near steady-state conditions). One would expect Equation (16) to overpredict the maximum stress, as the applied thermal profile did not have instantaneous changes in temperature. Slower thermal ramping allows stresses to begin to relax even as they are increasing during cooling. Maximum stress is therefore, lower than would result from a thermal profile with a quicker cool-down. Further discussion of the rate of

thermal ramping and the applicability of Equation (16) is contained in the following sections.

Transition Temperature Sensitivity

Let us assume for now that the recursive solution method accurately predicts stress in the example adhesive bond given the example thermal profile. If we could change the adhesive formulation so as to adjust the transition temperature independent of the other material properties, how would the development of residual stresses be affected? Could the glass transition temperature of a polymer be optimized to reduce the likelihood of debonding?

In order to examine the dependence of maximum stress on T_g, a series of numerical analyses were run for our example problem. The only parameter varied was T_g, (recall that CTE and a_T are referenced to T_g). Results of the analyses are plotted in Figure 7, along with the analytical curve from Equation (16). The dashed lines represent the values between which temperature is being cycled. The data show an insignificant stress level when T_g is very low and a maximum (4.30 MPa) when T_g is very high.

Each data point in Figure 7 represents stress in a material that has reached steady-state oscillation. There is, however, no indication of

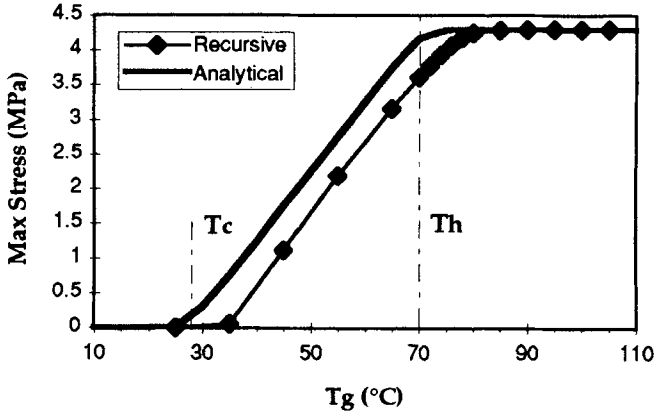

FIGURE 7 T_g sensitivity curve for cycling between T_c and T_h.

the number of cycles required to reach the steady state for materials with the different glass transition temperatures – information of great interest when attempting lifetime predictions. In Figure 8 are plotted the maximum stress levels developed on the inside of materials with different glass transition temperatures after different amounts of thermal cycling. Four different regions of T_g-sensitivity can be identified, here listed as found on the plot in Figure 8 from left to right:

Region I: Service temperature range exceeds T_g

In region I, the material is in its rubbery state for the entire span of the cyclic temperature profile. Stress relaxation occurs very quickly in viscoelastic materials at temperatures above the glass transition. Residual stress converges to its maximum value within one cycle, but at no point is that maximum a significanly large value. The stresses simply relax too quickly at both the hot and cold temperatures (Fig. 9).

Region II: Service temperature range spans T_g

In region II, the cycling limits span the transition temperature of the polymer. At the hot temperature relaxation rate is very high, so

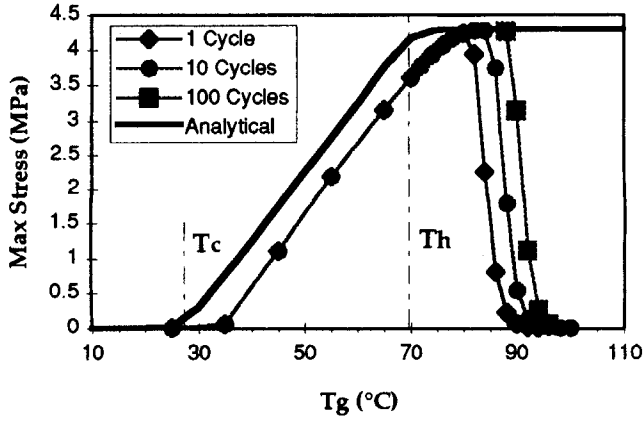

FIGURE 8 T_g sensitivity curve dependence on number of thermal cycles.

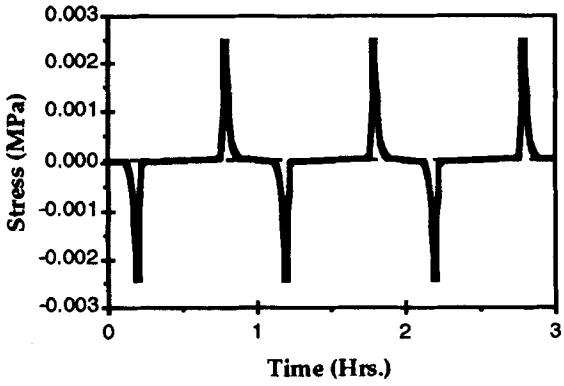

FIGURE 9 Stress *vs.* Time for T_g = 27°C.

convergence of stress build-up occurs after only one cycle. Unlike in region I, the material now becomes glassy during cooling, allowing some of the stress relaxation at the hot temperature to be frozen in as tensile stresses at the cold temperature (Fig. 10).

Region III: Service temperature range slightly below T_g

In region III, the material is glassy for the entire cycling span. However, the hot temperature is close enough to the glass transition temperature to allow for slow relaxation of stresses over many cycles.

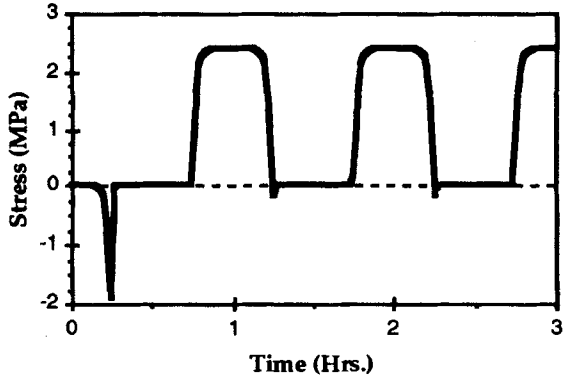

FIGURE 10 Stress *vs.* Time for T_g = 57°C.

Tensile residual stresses gradually accumulate (Fig. 11) to the maximum stress (steady-state) value.

Region IV: Service temperature range well below T_g

In region IV (Fig. 12), the hot temperature for cycling falls so far below the glass transition region that an inconsequential amount of stress build-up will occur during the entire lifespan of the application of interest. Where region IV begins will depend upon the intended lifetime of the application.

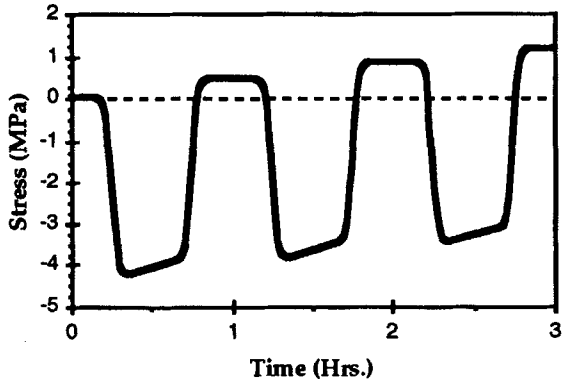

FIGURE 11 Stress *vs.* Time for $T_g = 87°C$.

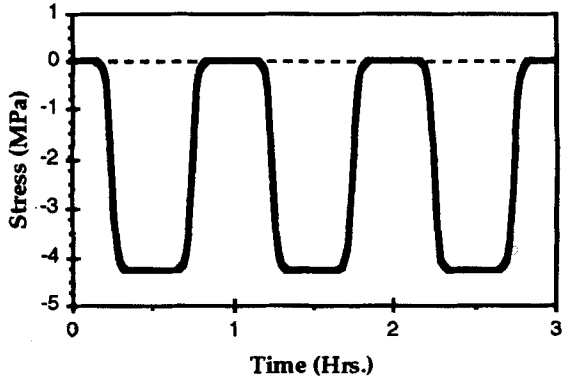

FIGURE 12 Stress *vs.* Time for $T_g = 117°C$.

Thermal Profile Sensitivity

The data points produced by the recursive equation are found to match the analytically-derived equation closely in regions I and IV, but to diverge greatly for any T_g in between (Fig. 7). This is not surprising since the numerical method accounts for the possibility of relaxation during thermal ramping, whereas the analytical method assumed near-instantaneous ramping. Cooling polymers more slowly will result in reduced residual stress levels; as the system cools and residual stresses begin to develop, there is more time for relaxation at the accelerated rates of the higher temperatures. The same principle should apply for thermal cycling. A thermal profile with rapid temperature changes would ultimately induce higher residual stresses more quickly than a profile with slower thermal changes. Figures 13 and 14 depict the predicted stress evolution given two different thermal profiles; the tanh-wave defined by Equation (12) and a sine wave with the same amplitude and period.

The stresses are clearly rising more slowly in Figure 13 than in Figure 14. In addition, the maximum stress level for the sine wave was predicted to be about 2.5%lower: 4.18MPa as compared with 4.27 MPa for the near-square wave input. In order to reveal the effect of thermal ramp rate on maximum stress level, a number of recursive solutions were again run, this time varying the steepness of the thermal

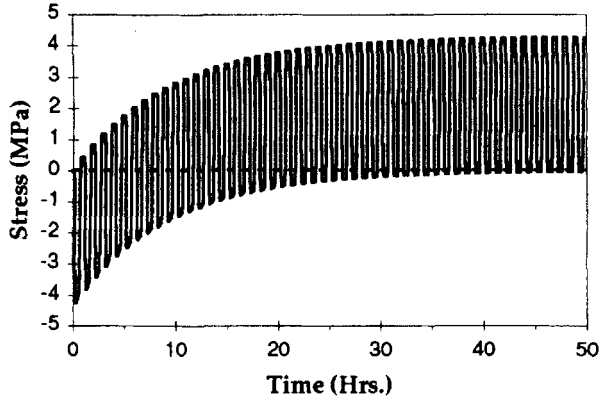

FIGURE 13 Stress development for a thermal cycle modeled as a tanh wave.

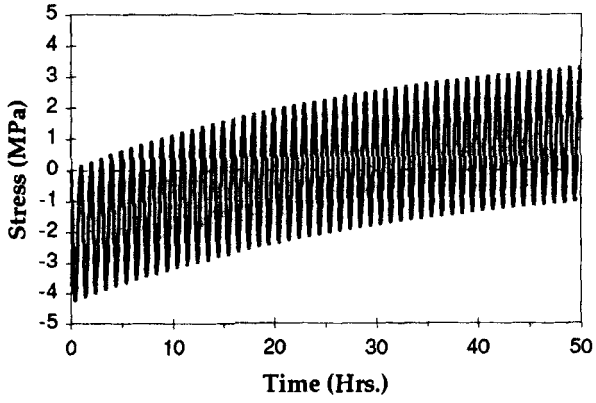

FIGURE 14 Stress development for a thermal cycle modeled as a sine wave.

ramp by defining the tanh-wave as before, but changing the denominator of the hyperbolic functions:

$$T(t) = 27 + 21.5\left[\text{Tanh}\left[\frac{t-900}{c}\right] - \text{Tanh}\left[\frac{t-2700}{c}\right]\right] \qquad (17)$$

Up to this point, c has been 120. Decreasing c makes the temperature changes steeper; a plot of the results is found in Figure 15.

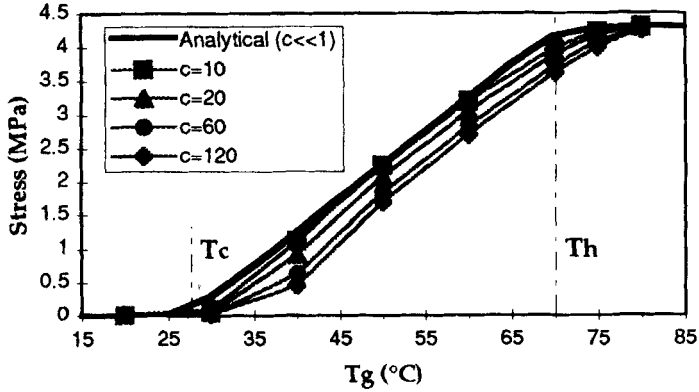

FIGURE 15 T_g sensitivity curve for different thermal profiles.

It was found that steeper thermal profiles cause more severe maximum stresses, especially in region II, but also to some extent in region III. The smaller the parameter c, the closer the thermal profile is to a square wave, and the closer the stress values come to the analytical equation for maximum stress prediction Eq. (16). For problems where operating range spans or nears the glass transition of a material, the particular shape of the thermal profile could be a significant consideration.

The preceding figures demonstrate that altering the T_g of the polymer will affect the maximum stress which will be encountered. One should recognize, however, that the initial residual stress is not independent of T_g, and this value will affect the magnitude of change associated with the stress evolution, and the exposure time needed to reach the predicted maximum stress. Changes in residual stress, however, would not necessarily affect the magnitude of the steady state stress eventually reached. The trends suggested by these figures are believed to be correct, but the reader should keep these cautions in mind when interpreting these results.

2-D FINITE ELEMENT SOLUTION

The Mesh

The more realistic 2-D geometry of an adhesive layer bonded between two substrates was analyzed using a finite element mesh and the software package ABAQUS[2]. Making use of symmetry, the mesh modeling a quarter of the bond (Fig. 16) was comprised of two layers of 35 eight-node parabolic elements each, with the two layers sharing nineteen nodes at the interface. The top layer was assigned to model a viscoelastic adhesive and the bottom layer was assigned to model an elastic substrate. The layers were made to have equal thickness to facilitate meshing. Plane stress conditions were assumed and boundary conditions were selected to enforce symmetry conditions.

ABAQUS is capable of evaluating stress development over time in systems containing viscoelastic elements by time stepping in a manner

[2]ABAQUS is a finite element product of Hibbitt, Karlsson, and Sorensen, Inc.

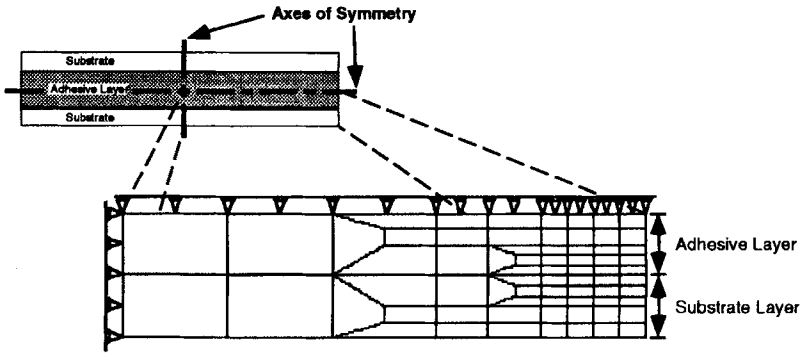

FIGURE 16 2-D finite element mesh of one quarter of a sandwich geometry.

similar to the recursive numerical method. This involves evaluating the full 2-D stress solution for the mesh at numerous time steps per cycle. The mesh was, therefore, chosen to be relatively coarse to minimize the processing load on the computer. Mesh density is not expected to affect the accuracy of the stress values near the left end of the mesh, where stresses are expected to be nearly constant. Where high gradients would be expected (near the right end), the stress magnitudes are not expected to be precise because of the coarseness of the mesh. Nonetheless, useful information can be gleaned from the results by observing how the stress levels in these elements change over time due to thermal cycling.

ABAQUS RESULTS

The finite element analysis was run using the same material properties for the adhesive as in the previous example. For the substrate, a modulus of 73 GPa and CTE of $25\times10^{-6}\ ^{\circ}C^{-1}$ were used. Figure 17 depicts the axial stress profile results returned by the finite element analysis after ten temperature cycles. Axial stress is nearly constant near the left end of the mesh (the axis of symmetry), and falls away to zero at the right side (the free end). Residual axial stress development in the 2-D geometry was found to follow the same trends as predicted by 1-D analysis. The tensile stresses at the cold temperature were

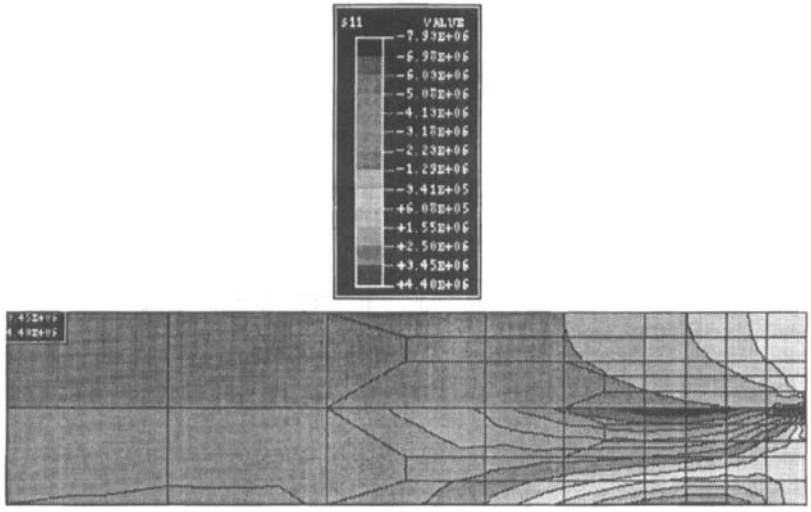

FIGURE 17 Axial stress distribution after ten thermal cycles.

found to increase over the number of cycles due to stress relaxation at the high temperature. The rate of stress development was nearly the same as predicted by the 1-D solution, similarly nearing steady-state conditions in 50 cycles.

One would expect the high axial stress gradients near the free end to be coupled with significant shear and peel stresses; indeed, this is a requirement of static equilibrium. Where axial stress is nearly constant (away from the free end), both shear and peel stresses should approach zero. The finite element results confirmed these suspicions (Figs. 18 and 19). Peel and shear stresses are localized near the end – where a crack is most likely to begin – and were found to increase incrementally in the same manner as axial stresses. The development of increasing tensile peel stresses is of critical importance. Tensile peel stresses would be expected to contribute to crack initiation and propagation at the ends of a bonded specimen, as has been observed experimentally.

Comparsion of 1-D and 2-D Anaysis Results

In the middle region of an adhesive bond, the adhesive layer is completely constrained by the substrates; stress is uniaxial and

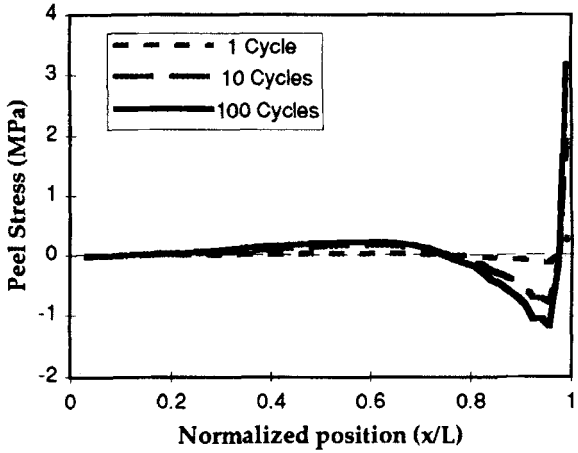

FIGURE 18 Peel stress distribution (cold temp.) for increasing numbers of thermal cycles.

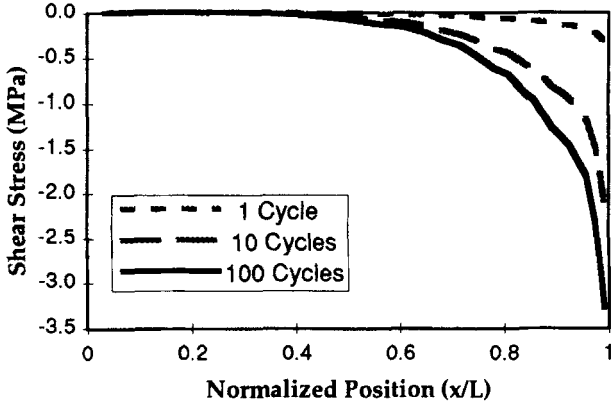

FIGURE 19 Shear stress distribution (cold temp.) for increasing numbers of thermal cycles.

effectively independent of position in the bond. Recall that assuming uniform uniaxial stresses was the simplification that allowed for the derivation of the recursive equation Eq. (12). Therefore, the only difference between the polymer in the center of a 2-D bond and the 1-D simplification is the constraint placed on total strain in the

material. Instead of being constrained to zero, total strain in the bonded polymer must match the thermal strain in the substrate.

By subtracting the CTE of the substrate (assumed to be independent of temperature) from the CTE of the polymer in the 1-D analysis, we should be able to get a solution that matches the prediction of stress in the center of the 2-D finite element solution. This proves to be the case; axial stress was predicted to be 3.21 MPa by adjusting the CTE in the 1-D recursive equation, very close to the 3.22 MPa value returned by the 2-D finite element plane stress solution. The 1-D equation is, therefore, sufficient to predict axial stress development in the center region of adhesive bonds and can be applied in place of the more complicated and time-consuming finite element analyses.

FRACTURE ANALYSIS

Let us consider a bonded sandwich geometry containing residual stresses as a result of thermal cycling. Crack initiation and propagation predictions are made by comparing the strain energy stored against the fracture toughness of the system. Applied strain energy release rates for a sandwich geometry give known residual stresses as can be derived using energy balance methods. Assuming that the substrates are relatively stiff compared with the adhesive, and recognizing that the strain energy release rate may be obtained by relieving the strain energy in a unit area of the adhesive layer, the available strain energy release rate can be expressed as:

$$G = \frac{h}{4E}\left[\left(\sigma_{xx}^2 + \sigma_{yy}^2 + \sigma_{zz}^2\right) - \nu\left(\sigma_{xx}\sigma_{yy} + \sigma_{yy}\sigma_{zz} + \sigma_{xx}\sigma_{zz}\right)\right] \quad (18)$$

For the case of a coating with only a single interface, the energy release rate would be double this value. Recall again that we have ceased considering the contribution of the substrates, so all variables in the equation refer to the adhesive layer only.

Simplification of Equation (18) for particular adhesive bond geometries will yield different results. Presented here are two different cases; it will be left to the reader to decide which (or what combination of the two) is most appropriate for any particular geometry of interest.

In all cases, σ is the value of axial stress in the center of the bond and h and E are thickness and stiffness of the adhesive.

Thick, Narrow Bond-Uniaxial Stress

A bond that is narrow in comparison with its bondline thickness will have a nearly uniaxial stress field built in by thermal cycling. Across the width of the interface, stresses will not develop significantly because the stress-free edges are close and the adhesive is able to contract in response to Poisson contraction from the axial stresses. Peel and shear stresses will be concentrated only at the ends. The 1-D simplification of a bond geometry was such a problem: only stress in the axial direction was non-zero. For the uniaxial stress case, Equation (18) reduces to the simple form:

$$G = \frac{h}{4E}\sigma^2 \tag{19}$$

Thin, Wide Bond-Equal Biaxial Stresses

A bond which is long and wide in comparison with its thickness will have equal residual biaxial stresses built in by thermal cycling. Because the bond is thin and wide, the adhesive cannot contract and stresses can develop across the width of the bond in the same manner as along the length. As with the thick, narrow bond, peel stresses and shear stresses will be concentrated in small regions near the edges.

When debonding occurs, the length of debonded region relative to thickness will determine the proper expression for G. When the debond is relatively short, the debonded region is under plane stress conditions, and hence still sustains stress in the transverse direction. The proper simplification of Equation (18) is the same as above; only strain energy stored in the material by axial stresses has been released, so Equation (19) will be sufficient to describe G. When the debonded length is much longer than the material is thick, energy stored in the material by transverse stresses can be released as well; the G equation becomes:

$$G = \frac{h(1-\nu)}{2E}\sigma^2 \tag{20}$$

A thin, wide bond with a relatively long crack will have greater G-values than the thick, narrow bond for a given stress level.

Using the recursive equation together with the appropriate strain energy release rate expression (from Eqs. (19) and (20)) for a given loading could, therefore, serve as a quick and easy way to calculate the effect of thermal cycling on applied strain energy release rate at the crack tip in an adhesively-bonded system.

DISCUSSION

Given the results presented, a plausible mechanism for the previously-described debonding and contraction behavior can be proposed. Initially, the bond is at the cold temperature and the residual stresses are minimal. Raising the temperature of the bond induces a compressive stress in the polymer because of the CTE mismatch between the adhesive and susbstrate. The higher temperature facilitates polymer chain mobility and relaxation of the compressive thermal stress. Cooling the system freezes in the structural changes; relaxation at the hot temperature is reflected in an increased tensile stress at the cold temperature. The low temperature inhibits flow, so the tensile stresses relax only very slowly. The initial stress state cannot be recovered before the next thermal cycle begins; there is now a net residual stress gain over one cycle. Thermal cycling thereby ratchets up the cold-side tensile stress with each cycle. Holding the specimen at the elevated temperature for an extended period of time and then cooling the specimen would also result in the elevated tensile stresses.

The applied strain energy release rate at the cold temperature at the tip of an interface crack in the bond has been shown to increase from thermal cycling as a result of increasing residual stresses. At some point, the available strain energy release rate becomes sufficient to initiate cracks spontaneously at the interfaces near the ends of the specimen. The cracks probably grow over time as a result of the fatigue loading induced by the cyclic thermal profile and the corresponding cyclic changes in residual stress state.

Once released from its constraints by debonding, the polymer layer contracts. Contraction occurs as the material returns to its new stress-

free strain. The change in stress-free strain from the initial condition is a result of viscoelastic flow that occurred in the polymer while under compressive stress at the hot temperature of each cycle.

The magnitude of changes in residual stress state at an adhesive interface are expected to be more serious under certain conditions. A summary is presented in Tables I and II. Table I lists the effects of different parameters on the rate of stress development. Table II summarizes the effects of different parameters on the magnitude of the built-in residual tensile stress.

Differing initial conditions will not change the results much; if the material is not initially stress-free at the low temperature, it simply starts with some thermal history. The trend of rising residual stresses will still occur, but it will take more or less time to rise to the maximum stress magnitude. The same is true if the initial temperature is not the

TABLE I Factors affecting rate of stress development

Rate of Stress Development	
Faster	*Slower*
Lower Characteristic Relaxation Time	Higher Characteristic Relaxation Time
Hot Temperature Closer to Glass Transition	Hot Temperature Further from Glass Transition
Steeper Thermal Ramps	More Gradual Thermal Ramps
Longer Time at Hot Temperature	Shorter Time at Hot Temperature

TABLE II Factors affecting maximum magnitude of built-in stresses

Magnitude of Maximum Stress	
Higher	*Lower*
Higher $\Delta\alpha$ Between Materials	Lower $\Delta\alpha$ Between Materials
Greater ΔT	Lesser ΔT
Higher T_g (if spanned by temperature range)	Lower T_g (if spanned by temperature range)
Steeper Thermal Ramps	More Gradual Thermal Ramps
Plane Strain	Plane Stress
Viscoelastic Fluid	Viscoelastic Solids
Higher Material Stiffness	Lower Material Stiffness

high or low temperature. At the the low temperature, the material will again start with initial residual stresses, this time from heating/cooling from the initial temperature.

Determining exactly when and how a crack is propagated for a given system requires knowing the critical fracture toughness (G_c) and fatigue fracture threshold strength as a function of temperature. After sufficient thermal exposure, stresses and strain energy release rate are highest at the cold temperature, suggesting that crack propagation could occur when the system is coldest. At the colder temperature, the stresses tend to open rather than close existing debonds. The work of Gorce *et al.* [22], however, reveals that toughness can rise as temperatures fall for some materials (in this case, polyurethanes). Probably crack growth in some bonds would occur during the thermal ramping, at a temperature between the maximum and minimum at which tensile stresses are of significant magnitude but toughness has not yet become very high.

CONCLUSION

Many practical adhesive bonds and coating applications are subjected to cyclic temperature conditions. At the higher service temperatures, compressive residual stresses in the polymeric adhesive or coating can relax significantly due to the thermal acceleration. When cooled to the lower service temperature, the residual stresses have evolved to increasingly larger tensile stresses which can relax very slowly because of the reduced molecular mobility. The asymmetry of relaxation can result in a continual rachetting of stresses toward a steady state situation in which relatively large tensile stresses exist at the cold temperature. Although the magnitude of this stress evolution can vary significantly for different material systems and thermal environments, the basic phenomenon is believed to be quite universal, dependent only on the presence of a bonded bimaterial system in which the materials have different coefficients of thermal expansion, and where at least one of the components exhibits viscoelastic behavior which is thermally accelerated. The phenonenon should, therefore, transcend the particular problem presented here, and apply to at least some degree to all adhesive bonds. The speed and severity of the phenomenon will

be determined by the parameters of each individual problem. Although this phenomenon will not be significant in many applications where the materials are used well below or well above the glass transition temperature, failure to account for this thermal rachetting in multimaterial systems thermally cycled in the vicinity of any transition temperature could lead to premature failures. Although the current paper has focused only on thermal cycles, changing moisture content (or other diluents) could also produce the same effect.

This work has developed some tools that could be used to predict the change in residual stress state due to thermal cycling, and the subsequent changes in strain energy release rate for bonded specimens. The recursive equation is one method to calculate simply the residual stress build-up in a bond given the thermal profile. With stresses known, simple fracture mechanics analysis yields predictions of the increase in applied strain energy release rate as a function of residual stress. It is hoped that these simple tools combined with a greater understanding of the role of viscoelasticity in the mechanics of a bonded joint will eventually lead to more durable design of adhesively-bonded applications in the future.

Acknowledgements

The authors would like to acknowledge the financial support of the Adhesive and Sealant Council, the Center for Adhesive and Sealant Science, and the National Science Foundation: Science and Technology Center (contract DMR 9120004), as well as the help of Mr. Raul Andruet with the details of ABAQUS programming.

References

[1] Timoshenko, S. P., "Analysis of Bi-Metal Thermostats", *J. Opt. Soc. Am.* **11**, 233–255 (1925).
[2] Erdogan, F., "Stress Distribution in Bonded Dissimilar Materials with Cracks", *J. Appl. Mech.* **32**, 403–410 (1965).
[3] Chen, W. T. and Nelson, C. W., "Thermal Stress in Bonded Joints", *IBM J. Res. Dev.* **23**(2), 657–660 (1989).
[4] Suhir, E., "Stresses in Bi-Metal Thermostats", *J. Appl. Mech.* **56**, 595–600 (1989).
[5] Suhir, E., "Interfacial Stresses in Bi-Metal Thermostats", *J. Appl. Mech.* **56**, 595–600 (1989).
[6] Losi, G. and Knauss, W., "Thermal Stresses in Nonlinearly Viscoelastic Solids", *J. Appl. Mech.* **59**, S43–S49 (1992).

[7] Struik, C., *Internal Stresses, Dimensional Instabilities, and Molecular Orientations in Plastics* (John Wiley and Sons, New York, NY, 1990).
[8] Kawada, H. and Ikegami, K., "Viscoelastic Properties of Resin for IC Plastic Packages and Residual stress", *JMSE Int. J.* Series I, **35**(2), 152–158 (1992).
[9] Lee, E. *et al.*, "Residual Stresses in a Glass Plate Cooled Symmetrically from Both Surfaces", *J. Am. Ceramic Soc.* **48**(9), 480–487 (1965).
[10] Lee, K. and Weitsman, Y., "Optimal Cool Down in Nonlinear Thermoviscoelasticity with Application to Graphite/PEEK (APC-2) Laminates", *J. Appl. Mech.* **61**, 367–374 (1994).
[11] Van Doorselaer, K. and DeZeeuw, K., "Relation between Delamination and Temperature Cycling Induced Failures in Plastic packaged Devices", *IEEE Trans. on Comp., Hyb. and Man. Tech.* **13**(4), 879–882 (1990).
[12] Chiou, B. *et al.*, "Temperature Cycling Effects between Sn/Pb Solder and Thick Film Pd/Ag conductor Metallization", *IEEE Trans. on Comp., Hyb. and Man. Tech.* **14**(1), 233–237 (1991).
[13] McDonald, G. and Hendricks, R., "Effect of Thermal Cycling on Zr_2O_2-Y_2O_3 Thermal Barrier Coatings", *Thin solid Films* **73**, 491–496 (1980).
[14] Kinloch, A. and Osiyemi, S. "Predicting the Fatigue Life of Adhesively-Bonded Joints", *J. Adhesion* **43**, 79–90 (1993).
[15] Jiang, W., "The Elastic-Plastic Analysis of Tubes-IV: Thermal Ratchetting", *J. Pres. Ves. Tech. Trans. of ASME* **114**(2), 236–245 (1992).
[16] Ryan, R. and Mall, S., "Cyclic Heating of a Layered Plate with an Interface Flaw", *J. Ther. Stresses* **42**, 33–46 (1991).
[17] Suresh, S., "Elastoplastic Analysis of Thermal Cycling: Layered Materials with Sharp Interfaces" *J. Mech. Phys. Solids* **42**(6), 979–1018 (1994).
[18] Dunn, M. and Taya, M., "Creep and Thermal Cycling Creep of Metal Matrix Composites", *Thermomechanical Behavior of Advanced Structural Materials*, AD-**34**/AMD-**73**, 33–46 (ASME, 1993).
[19] Lin, K. and Hwang, I., "Thermo-Viscoelastic Response of Graphite/Epoxy Composites", *J. Eng. Mat. Tech.* **110**, 113–116 (1988).
[20] Zienkiewicz, O. *et al.*, "A Numerical Method of Visco-elastic Stress Analysis", *Int. J. Mech. Sci.* **10**, 807–827 (1968).
[21] Williams, M., Landel, R. and Ferry, J., "The Temperature Dependence of Relaxation Mechanisms in Amorphous Polymers and Other Glass-Forming Liquids", *J. Am. Chem. Soc.* **77**, 3701–3706 (1955).
[22] Gorce, J., "Mechanical Hysteresis of a Polyether Polyurethane Thermoplastic Elastomer", *Polym. Eng. and Sci.* **33**(18), 1170–1176 (1993).